INVERSE MODELING OF A MULTISTEP OUTFLOW EXPERIMENT FOR DETERMINING HYSTERETIC HYDRAULIC PROPERTIES

S. Finsterle[1], T. O. Sonnenborg[2], and B. Faybishenko[1]

[1]Lawrence Berkeley National Laboratory
Earth Sciences Division, Mail Stop 90-1116
Berkeley, CA 94720

[2]Department of Hydrodynamics and Water Resources (ISVA)
Technical University of Denmark
2800 Lyngby, Denmark

ABSTRACT

A new, closed-form hysteretic model of the capillary pressure-saturation and relative permeability-saturation relationship has been implemented into ITOUGH2. The hysteretic capillary pressure function is based on the van Genuchten model, with a modified version of the dependent domain model of Mualem to describe the scanning curves. Hysteresis in the relative permeability relations is considered to be mainly a result of nonwetting fluid entrapment. The hysteresis model was used in combination with inverse modeling techniques to examine the potential of a simple drainage-imbibition experiment to determine hysteretic hydraulic properties.

INTRODUCTION

Hysteresis in the capillary pressure-saturation relationship, as well as entrapment of the nonwetting phase as a result of alternating drainage and imbibition events, has a significant impact on the distribution of moisture and contaminants in the subsurface [*Niemi and Bodvarsson*, 1988; *Essaid et al.*, 1993; *Deng and Pantazidou*, 1998]. Hysteresis in water retention properties of soils may be attributed to several factors, such as [*Hillel*, 1982]:

* Geometric nonuniformity of individual pores, resulting in the "inkbottle effect";
* Different spatial connectivity of pores during drying and wetting;
* Variations in liquid-solid contact angle;
* Air entrapment.

Some or all of these factors may act simultaneously, which makes it difficult to separate the individual effects based on observed hysteretic data. Furthermore, hysteresis depends on the velocity, with which the saturation changes occur.

While the presence of hysteresis in porous materials and its importance for predicting multiphase flow is well recognized, only a limited number of simulation studies using hysteretic capillary pressure functions have been performed [*Lenhard and Parker*, 1987; *Kool and Parker*, 1988]. Furthermore, most of these studies neglect hysteresis in the relative permeability functions, which may strongly influence the behavior of the nonwetting phase [*Sonnenborg et al.*, 1998].

Predicting hysteretic behavior by means of numerical simulation requires (1) selecting an appropriate parametric model describing the hysteretic hydraulic properties of the porous medium, and (2) estimating the parameters of the hysteretic capillary pressure and relative permeability functions. Both steps are complex and require handling strongly nonlinear effects, especially during saturation-path reversals.

The objectives of this study are (1) to implement a hysteretic capillary pressure and relative permeability model into TOUGH2, and (2) to evaluate the potential of inverse modeling techniques to derive soil hysteretic properties from a transient drainage-imbibition experiment.

HYSTERESIS MODEL

Hysteretic capillary pressure and relative permeabilities depend on the saturation-desaturation history. More specifically, the functional forms and their parameters change whenever a saturation reversal point is reached, i.e., when the saturation transient switches from imbibition to drainage or vice versa. Note that

at any given point in time, different volume elements of the porous material may undergo drainage or imbibition, which requires the numerical model to keep track of the saturation history in each individual gridblock.

In our model, the main branches of the hysteretic capillary pressure-saturation relation are described using the expression proposed by *van Genuchten* [1980]:

$$P_c = -\frac{1}{\alpha^\gamma}\left[\left(\frac{S_l - S_{lr}}{1 - S_{lr} - S_{gr}^\Delta}\right)^{-1/m^\gamma} - 1\right]^{1/n^\gamma} \quad (1)$$

where $P_c = P_l - P_g$ is the capillary pressure, S_l is the liquid saturation, S_{lr} and S_{gr}^Δ are the residual liquid and gas saturations, respectively, α, m and n are curve shape parameters with $m = 1 - 1/n$, and the superscript γ refers to drying (d) or wetting (w). The residual gas saturation S_{gr}^Δ is not considered to be a constant, but depends on the saturation at which reversal from drainage to imbibition occurs. The lower the liquid saturation at the reversal point, the more gas is entrapped because it is forced into progressively smaller pores during drainage; the amount of gas left behind as isolated islands during the imbibition process increases with decreasing reversal saturation S_l^Δ as follows:

$$S_{gr}^\Delta = \frac{1 - S_l^\Delta}{1 + R_{gl}(1 - S_l^\Delta)} \quad (2)$$

where

$$R_{gl} = \frac{1}{S_{gr}^{max}} - \frac{1}{1 - S_{lr}} \quad (3)$$

The maximum amount of entrapped gas, S_{gr}^{max}, which is an input parameter, is asymptotically reached when following the main wetting curve. This model describes the amount of air entrapped under both unsaturated and quasi-saturated conditions, accounting for the change in the volume fraction of air in a free, connected state, and air entrapped within the liquid phase [*Chahal*, 1969; *Faybishenko*, 1995].

The history-dependent entrapped gas saturation as well as its inclusion in the relative permeability curves are the new feature added

to the hysteretic van Genuchten model described by *Niemi et al.* [1988].

The scanning curves are based on a modified version of the dependent domain model of *Mualem* [1984] as described in *Niemi and Bodvarsson* [1988]. The first-order wetting scanning curve is given by

$$S_l = S_l^d(P_c^\Delta) + \frac{[S_{lc} - S_l^d(P_c^\Delta)]}{[S_{lc} - S_l^w(P_c^\Delta)]}[S_l^w(P_c) - S_l^w(P_c^\Delta)] \quad (4)$$

where P_c^Δ is the capillary pressure at the reversal point from the main drying curve to the first-order wetting curve, S_l^d and S_l^w are the liquid saturations evaluated on the main drying and wetting curves, respectively, and $S_{lc} = 1 - S_{gr}^\Delta$ is the so-called critical liquid saturation. Equation (4) is used to solve for $S_l^w(P_c)$, which is the only unknown in the expression. Note that S_l is the primary variable known from the solution of the governing two-phase flow equations, the reversal capillary pressure P_c^Δ is saved when the reversal takes place, and $S_l^d(P_c^\Delta)$ and $S_l^w(P_c^\Delta)$ can be solved by inverting Equation (1). Once $S_l^w(P_c)$ is evaluated, the corresponding hysteretic capillary pressure P_c can be solved from the main wetting curve using (1).

Second-order drying curves are evaluated using

$$S_l = S_l^\Delta - \frac{[S_{lc} - S_l^d(P_c^+)]}{[S_{lc} - S_l^w(P_c^+)]^2} \cdot$$

$$[S_{lc} - S_l^w(P_c)][S_l^w(P_c^\Delta) - S_l^w(P_c)] \quad (5)$$

where S_l^Δ is the liquid saturation at the reversal point from the first-order wetting scanning curve to the second-order drying scanning curve, and P_c^+ is the capillary pressure for which $S_l^d(P_c^+)$ equals S_l. Again, the only unknown in Equation (5) is $S_l^w(P_c)$; the capillary pressure P_c^+ can be found from the expression for the main drying curve. Solving (5) for $S_l^w(P_c)$ produces a parabolic equation with two solutions. *Niemi et al.* [1987] showed that the physically meaningful solution, $S_l^w(P_c) < S_l^w(P_c^\Delta)$ can be readily detected.

Higher-order scanning curves are approximated as semilog-straight lines between the last two reversal points, leading to hysteretic loops that become narrower with increasing order, and that meet at the appropriate reversal points.

Assuming that hysteresis in the relative permeability functions is mainly a result of non-wetting fluid entrapment, we adopt the approach described by *Lenhard and Parker* [1987]. They modified *Mualem*'s [1976] predictive model by including a term that accounts for the reduction in liquid relative permeability as a result of gas-phase entrapment. The amount of entrapped gas lies between zero and S_{gr}^{Δ}, and is assumed to be a linear function of the effective liquid saturation. The final expression for the hysteretic relative permeability includes a sum of terms representing the saturation history from the starting point to the current position. For details, the reader is referred to *Lenhard and Parker* [1987].

A total of six parameters (S_{lr}, S_{gr}^{max}, α^d, α^w, n^d, n^w) have to be determined for this specific hysteresis model. The experimental, point-wise determination of hysteretic capillary pressure and relative permeability functions is very difficult and time consuming. We propose to use inverse modeling to estimate hysteretic hydraulic properties from transient laboratory experiments or field tests. In the following section, we summarize the elements of a formal parameter estimation procedure, and then apply the method to synthetically generated data that exhibit relatively strong hysteresis effects.

INVERSE MODELING

Solving the inverse problem is usually defined as the estimation of parameters by calibrating a model against observed data. We follow the standard procedure [*Beck and Arnold*, 1977] and minimize some measure of the differences between the observed and predicted system responses, which are assembled in the residual vector $\mathbf{r}$ with elements

$$r_i = y_i{}^* - y_i(\mathbf{p}) \qquad (6)$$

Here, $y_i{}^*$ is an observation at a given point in space and time, and y_i is the corresponding model prediction, which depends on the vector $\mathbf{p}$ of the unknown model parameters. In

inverse modeling, the distribution of the final residuals is expected to be consistent with the distribution of the measurement errors, provided that the true system response is correctly identified by the model. If the error structure is assumed to be Gaussian, the objective function to be minimized can be inferred from maximum-likelihood considerations to be the sum of the squared residuals weighted by the inverse of the covariance matrix $\mathbf{C}_{yy}$:

$$Z(\mathbf{p}) = \mathbf{r}^T \mathbf{C}_{yy}^{-1} \mathbf{r} \qquad (7)$$

An iterative procedure is needed to minimize Equation (7). The Levenberg-Marquardt modification of the Gauss-Newton algorithm [*Beck and Arnold*, 1977] was found to be suitable for our purposes [*Finsterle*, 1997b].

Under the assumption of normality and linearity, a detailed error analysis of the final residuals and the estimated parameters can be conducted. For example, the covariance matrix of the estimated parameter set is given by

$$\mathbf{C}_{pp} = s_0^2 (\mathbf{J}^T \mathbf{C}_{yy}^{-1} \mathbf{J})^{-1} \qquad (8)$$

where $\mathbf{J}$ is the Jacobian matrix at the solution. Its elements are the sensitivity coefficients of the calculated system response with respect to the parameters:

$$J_{ij} = -\frac{\partial r_i}{\partial p_j} = \frac{\partial y_i}{\partial p_j} \qquad (9)$$

In Equation (8), s_0^2 is the estimated error variance, a goodness-of-fit measure given by

$$s_0^2 = \frac{\mathbf{r}^T \mathbf{C}_{yy}^{-1} \mathbf{r}}{M - N} \qquad (10)$$

where M is the number of observations and N is the number of parameters. The inverse modeling formulation outlined above is implemented in a computer program named ITOUGH2 [*Finsterle*, 1997a,b]. ITOUGH2 provides estimates of any TOUGH2 input parameter [*Pruess*, 1991] based on any type of observation, for which a corresponding TOUGH2 output variable can be calculated. We use ITOUGH2 to analyze synthetically generated data from a multistep drainage-imbibition experiment, and to examine the potential of this experiment for estimating hysteretic hydraulic properties.

APPLICATION

Model Development

Figure 1 shows a schematic of a flow cell designed for radial drainage-imbibition experiments on soil samples. A vacuum can be applied at the central ceramic cylinder for soil water extraction. The apparatus is instrumented with a vial to measure the cumulative water discharge through the central cylinder. Moreover, a tensiometer for water potential measurements is installed near the outer wall of the flow cell. A similar configuration is used for water injection.
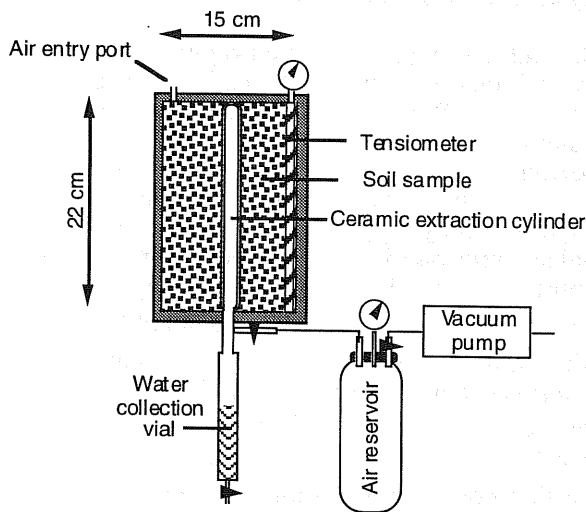

Figure 1. Schematic of apparatus for radial flow experiment.

Neglecting the minor effects of gravity, a one-dimensional radial model was developed, taking into account the impedance of the ceramic cylinder. A set of hysteretic hydraulic properties was assumed (see Table 1, Column 2), and synthetic cumulative outflow and capillary pressure data were generated for a multistep drainage-imbibition experiment, in which a suction pressure of -90 kPa was first applied at the extraction cylinder for 3 days. Subsequently, water was supplied without overpressure through the central cylinder for a 3-day period, leading to entrapment of air in the soil sample. Another drainage-imbibition cycle was simulated for time periods of 6 and 18 hours, respectively. Gaussian noise was added to the synthetic, true system response to simulate measurement errors. The standard deviations for the noise added to the capillary pressure and cumulative outflow data were 5 kPa and 25 ml, respectively.

The true hysteretic capillary pressure and relative permeabilities at the outer wall of the flow cell are visualized in Figures 2 and 3, respectively. Note that Figures 2 and 3 do not render the actual observed data; the measurements are shown as symbols in Figures 4 through 6. Nevertheless, an approximation of the hysteretic capillary pressure curve could be obtained by plotting the tensiometer data against the average soil saturation as calculated from the cumulative outflow data. Because of the averaging, this procedure would yield only an approximation of the curve shown in Figure 2, which represents the actual hysteretic loop encountered by the tensiometer. The hysteresis in the gas and liquid relative permeabilities cannot be directly observed during a transient experiment.

Inversions

Three different models have been calibrated against the synthetic data. The first model uses standard, non-hysteretic van Genuchten functions, i.e., $\alpha^d = \alpha^w = \alpha$, $n^d = n^w = n$, and $S_{gr}^{max} = S_{gr}$. The second model allows for hysteresis, but neglects the effects of air entrapment by setting $S_{gr}^{max} = 0$. Finally, the data are matched using the full hysteresis model. The matches to the capillary pressure and cumulative outflow data obtained with the three models are shown in Figures 4 through 6; the resulting parameter sets are summarized in Table 1.
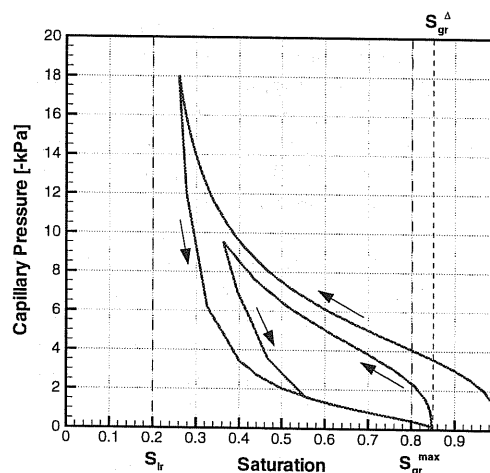
Figure 2. Computed hysteretic capillary pressure path at the outer wall of the flow cell.
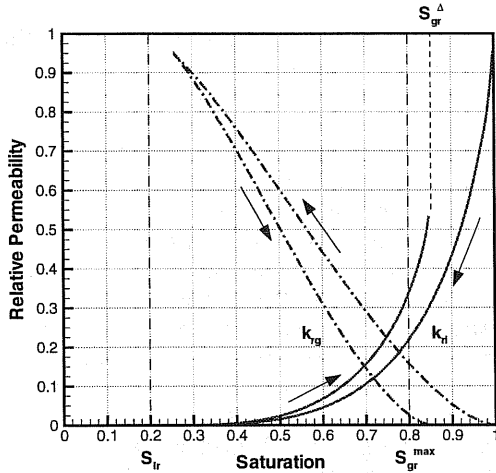
Figure 3. Computed gas and liquid relative permeability paths at the outer wall of the flow cell.

Table 1. True and Estimated Parameter Sets

Parameter	True	No hys-teresis	No air entrap-ment	Hys-teresis
$\log(k_{abs}$ [m^2])	-12.00	-11.64	-11.92	-11.97
$\log(1/\alpha^d$ [Pa])	3.69	3.41	3.71	3.70
$\log(1/\alpha^w$ [Pa])	3.00	-	2.43	2.98
n^d	3.00	2.13	3.14	3.01
n^w	2.00	-	1.33	1.97
S_{lr}	0.20	0.16	0.21	0.20
S_{gr}^{max}	0.20	0.40[#]	-	0.18

[#] At specified upper boundary

Discussion

Matching data that exhibit hysteretic effects with a nonhysteretic model yields an imperfect match. While the estimated α and n parameters are within the bounds of the respective drying and wetting values of the hysteretic model, an unreasonably high residual gas saturation is required to obtain near-zero capillary pressures and reduced flow rates during imbibition. Furthermore, the absolute permeability is overestimated by more than a factor of 2, to partly compensate for the reduced effective liquid permeability and the reduced driving force during drainage, which stems from the lower capillary pressure gradient.

An almost perfect match to the observed data is obtained with the second model (see Figure 5). This result may be surprising given that the hysteretic model does not include the effect of air entrapment, which is believed to

have a strong impact on system behavior [*Faybishenko*, 1995]. There are several explanations for this result First, while S_{gr}^{max}, which describes air entrapment, may be a sensitive parameter affecting forward predictions, its effect on the observed data, which are used during inverse modeling, may not be uniquely distinguishable. In other words, the lack of a formal inclusion of air entrapment in the model can be partly compensated for by adjusting other parameters, especially those describing the wetting curves. Since a reasonable match was obtained despite fixing S_{gr}^{max} at zero, it can be expected that it will be difficult to identify each of the parameters of the hysteretic model based on the available data.

Second, the impact of air entrapment becomes more important towards the end of a saturation period. While the cumulative outflow continuously declines during the imbibition periods (see Figure 5), the one obtained with the full hysteresis model (see Figure 6) asymptotically approaches a final, non-zero value representing the total amount of entrapped air. Therefore, it is likely that the experiment is inappropriate to identify S_{gr}^{max}. The design of the experiment could be improved by extending the imbibition periods, as suggested by the increase in the sensitivity coefficients $|\partial q(t) / \partial S_{gr}^{max}|$ for $t \to 6$ days. Furthermore, approaching the main wetting curve by extending the drainage period also help better identify S_{gr}^{max}.

Finally, neglecting air entrapment may not be significant for this soil and the prevailing test conditions. The main wetting branch of the capillary pressure curve is not strongly affected by S_{gr}^{max}, and the differences in the relative liquid permeabilities have only an impact during a small period of the entire test duration.

The hysteretic hydraulic properties are accurately identified when using the correct hysteresis model. Deviations from the true values are a result of the noise in the data. Note, however, that the relatively strong parameter correlations may lead to non-unique solutions when analyzing real data, i.e., when the assumed hysteresis model is unlikely to perfectly mimic the actual hysteretic behavior.

The discussion above emphasizes the importance of a careful test design, which should also be based on synthetic inversions rather

than on forward modeling alone [*Finsterle and Faybishenko*, 1997]. If S_{gr}^{max} is considered a key parameter for making model predictions, the experiment should be designed to maximize the sensitivity of the observed variables with respect to S_{gr}^{max}. The correlation of S_{gr}^{max} to the other parameters should be reduced to obtain an independent estimate of sufficiently low uncertainty.
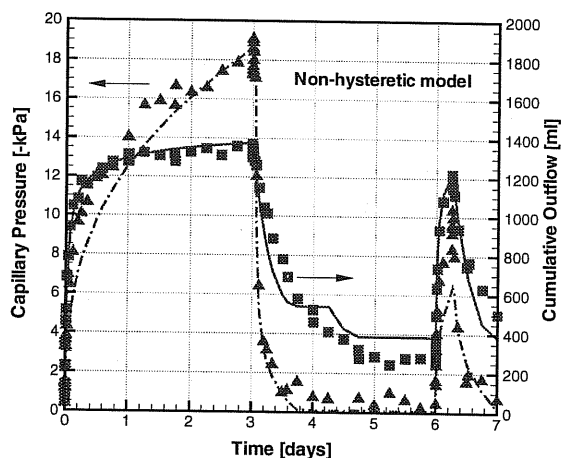

Figure 4. Comparison between observed (symbols) and calculated (lines) capillary pressure and cumulative outflow. Nonhysteretic model.
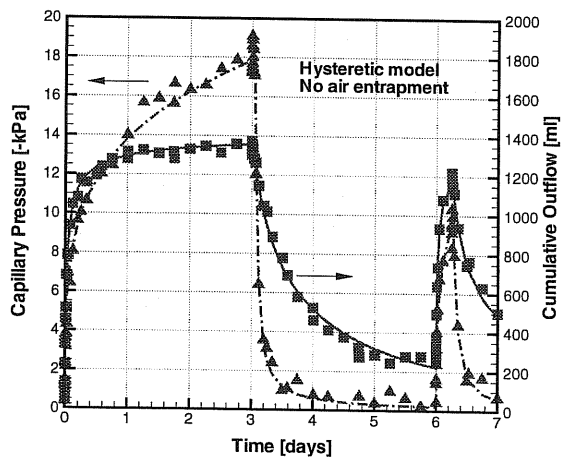

Figure 5. Comparison between observed (symbols) and calculated (lines) capillary pressure and cumulative outflow. Hysteretic model without air entrapment.
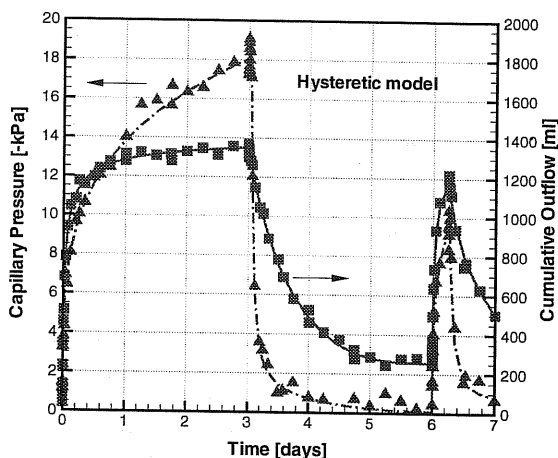

Figure 6. Comparison between observed (symbols) and calculated (lines) capillary pressure and cumulative outflow. Hysteretic model.

We proceed with a discussion of some of the statistical parameters calculated by ITOUGH2. First, the goodness-of-fit as measured by the estimated error variance (see Equation (10)) provides an overall assessment of the match obtained. Table 2 shows that while the correct hysteresis model realizes the best match according to the goodness-of-fit criterion (the differences are statistically significant on the 95% confidence level), it may not be justified to estimate all parameters of the full hysteresis model. The A-optimality criterion, which is the sum of the estimation variances scaled by the square of the parameter values, in fact favors the hysteresis model that does not include air entrapment. Estimating an additional parameter, i.e., S_{gr}^{max}, leads to higher overall correlations and thus larger estimation uncertainties, which cannot be fully compensated by the improvement of the fit.

Table 2. Estimated Error Variance and A-Optimality Criterion

Model	Number of parameters	Estimated error variance	A-optimality criterion[#]
No hysteresis	5	9.52	0.0081
Hysteresis no air entrapment	6	1.71	0.0008
Hysteresis	7	0.98	0.0014

[#] Trace of scaled estimation covariance matrix $\mathbf{C}_{pp}$

255

CONCLUDING REMARKS

A new hysteresis module has been developed for use with ITOUGH2. With a limited set of parameters, hysteresis in the capillary pressure curve as well as the gas and liquid relative permeability functions is modeled, taking into account history-dependent entrapment of the nonwetting phase. The module was used to generate synthetic data of a multistep drainage-imbibition experiment using radial flow geometry.

Parameter estimation using ITOUGH2 demonstrates the flexibility of inverse modeling concepts to extract information about hysteretic soil properties from a combined analysis of transient data, such as cumulative outflow and capillary pressure measurements. It becomes obvious, however, that the experiment has to be carefully designed to explore the full saturation range using alternating drying and resaturation events.

We are currently running a laboratory experiment to obtain hysteretic data that will be analyzed using the approach developed in this paper.

REFERENCES

Beck, J. V. and K. J. Arnold, *Parameter Estimation in Engineering and Science*, John Wiley & Sons, New York, 1977.

Chahal, R. S., "Effect of Temperature and Trapped Air on Matric Suction," *Soil Sci.*, *100*(4), 262-266, 1965.

Deng, Y. and M. Pantazidou, "Effects of Hysteresis in Capillary Pressure-Saturation Relationships on Predicting LNAPL Mobility," *Proceedings*, XII International Conference on Computation Methods in Water Resources, Crete, Greece, June 15-19, 1998.

Essaid, H. I., W. N. Herkelrath and K. M. Hess, "Simulation of Fluid Distributions Observed at a Crude Oil Spill Site Incorporating Hysteresis, Oil Entrapment, and Spatial Variability of Hydraulic Properties," *Water Resour. Res.*, *29*(6), 1753-1770, 1993.

Faybishenko, B., "Hydraulic Behavior of Quasi-Saturated Soils in the Presence of Entrapped Air: Laboratory Experiments," *Water Resour. Res.*, *31*(10), 2421-2435, 1995.

Finsterle, S., *ITOUGH2 Command Reference, Version 3.1*, Report LBNL-40041, Lawrence Berkeley National Laboratory, Berkeley, Calif., 1997a.

Finsterle, S., *ITOUGH2 Sample Problems*, Report LBNL-40042, Lawrence Berkeley National Laboratory, Berkeley, Calif., 1997b.

Finsterle, S. and B. Faybishenko, "Design and Analysis of an Experiment to Determine Hydraulic Parameters of Variably Saturated Porous Media," Report LBNL-40245, Lawrence Berkeley National Laboratory, Berkeley, Calif., (submitted to *Advances in Water Resour.*), 1997.

Hillel, D., *Introduction to Soil Physics*, Academic Press, Inc., San Diego, Calif., 1982.

Kool, J. B. and J. C. Parker, "Analysis of the Inverse Problem for Transient Unsaturated Flow," *Water Resour. Res.*, *24*(6), 817-830, 1988.

Lenhard, R. J. and J. C. Parker, "A Model for Hysteretic Constitutive Relations Governing Multiphase Flow, 2. Permeability-Saturation Relations," *Water Resour. Res.*, *23*(12), 2197-2206, 1987.

Mualem, Y. "Hysteretical Models for Prediction of the Hydraulic Conductivity of Unsaturated Porous Media," *Water Resour. Res.*, *12*(6), 1248-1254, 1976.

Mualem, Y., "A Modified Dependent Domain Theory of Hysteresis," *Soil Sci.*, *137*(5), 283-291, 1984.

Niemi, A. and G. S. Bodvarsson, "Preliminary Capillary Hysteresis Simulation in Fractured Rocks, Yucca Mountain, Nevada," *J. Contam. Hydrol.*, *3*, 277-291, 1988.

Niemi, A., G. S. Bodvarsson and K. Pruess, *Incorporation of the Capillary Hysteresis Model HYSTR into the Numerical Code TOUGH*, Report LBL-23592, Lawrence Berkeley Laboratory, Berkeley, Calif., 1987.

Pruess, K., *TOUGH2—A General-Purpose Numerical Simulator for Multiphase Fluid and Heat Flow*, Report LBL-29400, Lawrence Berkeley Laboratory, Berkeley, Calif., 1991.

Sonnenborg, T. O., M. B. Butts, and S. Finsterle, "Estimation of Hysteretic Two-Phase Hydraulic Properties From Transient Flow Experiments," Report, Technical University of Denmark, 1998.

van Genuchten, M. Th., "A Closed-Form Equation for Predicting the Hydraulic Conductivity of Unsaturated Soils," *Soil Sci. Soc. Am. J.*, *44*(5), 892-898, 1980.